Commensurate-incommensurate transitions and the Lifshitz point in the quantum asymmetric clock model*

Steven F. Howes
The James Franck Institute, The University of Chicago, 5640 South Ellis Avenue, Chicago, Illinois 60637
(Received 12 August 1982; revised manuscript received 2 November 1982)

The asymmetric three-state clock model is studied in the context of a one-dimensional quantum Hamiltonian. Series expansions are used to investigate the commensurate-incommensurate transition and the incommensurate-liquid Kosterlitz-Thouless transition. Evidence is presented for a Lifshitz point at which the critical indices α, β, and γ are Potts-type, while the mass-gap index appears to take its Ising value, $\nu=1$.

I. INTRODUCTION

The asymmetric clock model introduced by Ostlund[1] describes certain features of the commensurate-incommensurate *(C-I)* transition observed in two-dimensional experimental systems, such as xenon monolayers absorbed on copper substrates.[2] Following Villain and Bak's[3] treatment of the anisotropic next-nearest-neighbor Ising (ANNNI) model, a low-temperature free-fermion approximation was used[1] to deduce properties of the striped incommensurate phase and the *C-I* transition. According to this method, a meandering domain wall is identified with a free fermion moving in one dimension. It was predicted that the incommensurate phase melts to a disordered phase via the unbinding of dislocation pairs. For the three-state model, one then expects a Lifshitz point from which a *C-I* line, a Kosterlitz-Thouless line, and a Potts line emerge. We have recently analyzed a self-dual version of this model[4] and find the Lifshitz point has a rather striking signature: The thermodynamic exponents α, β, and γ take the values characteristic of the Potts model, and the mass-gap index ν is equal to one, as in the Ising model.

The asymmetric clock model, in its one-dimensional quantum form, is defined by the Hamiltonian

$$H=-\sum_n \cos(ap_n)+\beta\cos(\theta_{n+1}-\theta_n-\Delta)a\ , \qquad a=\frac{2\pi}{3}\ . \tag{1.1}$$

The operators θ and p each have three eigenvalues 0, 1, and 2, and satisfy the commutation relation

$$e^{-ia\theta_n}e^{iap_m}e^{ia\theta_n}=e^{ia\delta_{nm}}e^{iap_m}\ . \tag{1.2}$$

The coupling constant β is proportional to the inverse temperature. At $\Delta=0$, (1.1) is the Hamiltonian of the three-state Potts model.

The quantum Hamiltonian (1.1) may be derived by considering the extreme anisotropic limit of the two-dimensional (2D) classical Hamiltonian

$$\mathscr{H}=-\sum_{x,t}K_t\cos(\theta_{x,t+1}-\theta_{x,t})a +K_x\cos(\theta_{x+1,t}-\theta_{x,t}-\Delta)a\ , \tag{1.3}$$

where $\theta_{x,t}=0,1,2$, i.e., in the limit $K_x\to 0$, $K_t\to\infty$ such that $\beta=K_x e^{3/2K_t}$ is finite.

In this paper, high- and low-temperature series for the free energy, magnetization, susceptibility, and the q-dependent mass gap are analyzed. This analysis leads to the phase diagram shown in Fig. 1. The main features are as follows:

(1) Lifshitz points B and B' at which α, β, and γ are Potts-type, and ν appears to be given by $\nu=1$.

(2) Commensurate-incommensurate lines BC and CB' of the type previously studied in striped incommensurate systems.[5]

(3) A line of Kosterlitz-Thouless transitions BB' separating the incommensurate and disordered phases. The mass-gap wave vector varies continuously along this line.

(4) Critical lines AB and $B'A'$ belonging to the three-state Potts universality class.

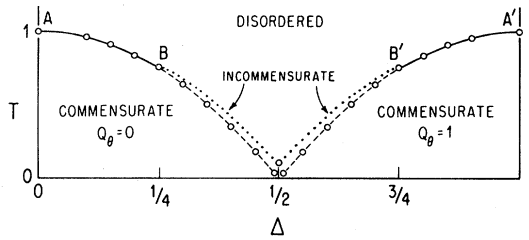

FIG. 1. Phase diagram derived from the Hamiltonian, Eq. (1.1).

Details of the numerical study are presented in the following sections. References 1 and 4 contain detailed explanations of the theoretical methods employed to study the Hamiltonian (1.1).

II. RESULTS FROM SERIES ANALYSIS

A. Outline of method and exact limits

Perturbative expansions for the eigenvalues of the Hamiltonian are related to high-temperature series for the thermodynamic quantities derived from the classical model (1.3). For example, the specific heat is obtained by differentiation of the ground-state energy:

$$C=\frac{\partial^2}{\partial\beta^2}E_0(\beta,\Delta)\ . \tag{2.1}$$

The expectation value of the disorder operator

$$D=\sum_n \cos\left[\sum_{m\le n} ap_m\right]$$

is the appropriate "order" parameter in the small-β, high-temperature phase. The corresponding susceptibility is given by

$$\chi=\langle D^2\rangle-\langle D\rangle^2=\frac{\partial}{\partial h}\langle D\rangle_{H+hD}\,|_{h=0}\ , \tag{2.2}$$

where $\langle D\rangle_{H+hD}$ denotes the expectation value of D with respect to the ground state of $H+hD$.

The mass gap is essential for studying transitions involving incommensurate phases. It describes the asymptotic decay of correlations in the "time" direction, i.e.,

$$\langle e^{ia(\theta_{x,t+r}-\theta_{x,t})}\rangle\sim e^{-mr}\ , \tag{2.3}$$

where m is the difference between the first excited- and ground-state energies. According to Bloch's theorem, we know that the excited states of H can be labeled by a wave vector q. At $\beta=0$, the appropriate translationally covariant first excited state is

$$|\psi_1\rangle_{\beta=0}=\sum_n |p_n=P\neq 0;p_{m\neq n}=0\rangle e^{-ianq}\ , \qquad |q|\le\tfrac{3}{2}\ . \tag{2.4}$$

The total "internal momentum" $P=\sum_n p_n$ has eigenvalues 0, 1, and 2, and is conserved because the interaction part of H depends only on the difference $\theta_{n+1}-\theta_n$. Thus the mass gap obtained perturbatively from (2.4) depends on the continuous parameter q. The value of q which makes $m(q)$ vanish at the smallest value of β defines the critical wave vector q_c and determines the critical coupling β_c, i.e.,

$$m(q_c)\sim(\beta_c-\beta)^{\nu}\ . \tag{2.5}$$

As in previous work,[4] one argues that the q_c deduced from the high-temperature series is the pitch of the low-temperature phase, at the critical point. This pitch Q_θ, which is defined by the periodicity of the correlation function, describes the phase modulation in the space direction:

$$\langle e^{ia(\theta_{x+r,t}-\theta_{x,t})}\rangle\sim e^{iarQ_\theta}\ . \tag{2.6}$$

When q_c locks in at a rational number and is therefore independent of Δ, the corresponding low-temperature phase is called commensurate. In our case, the commensurate phases have Q_θ being an integer. An incommensurate phase is signaled by the continuous variation of q_c with Δ. In this case, Q_θ also varies continuously and can be irrational and hence incommensurate with the lattice.

Low-temperature series are most conveniently derived from the dual version of (1.1). The dual variables are defined on the bonds of the original lattice. If $\bar{n}$ refers to the bond between sites n and $n+1$, the dual Hamiltonian is given by

$$H_D=-\sum_n \cos(p_{\bar{n}}-\Delta)a + T\cos(\theta_{\overline{n+1}}-\theta_{\bar{n}})a\ , \tag{2.7a}$$

$$p_{\bar{n}}=\theta_{n+1}-\theta_n,\quad \theta_{\bar{n}}=\sum_{m\le n} p_m,\quad T=\beta^{-1}\ . \tag{2.7b}$$

The magnetization is obtained by calculating the expectation value of the operator

$$O=\sum_n \cos\left[a\sum_{m\le n} p_{\bar{m}}\right]\ ,$$

and the susceptibility is derived from an expression like (2.2).

The low-temperature mass gap now describes the asymptotic decay of disorder operator correlations:

$$\left\langle \exp ia\sum_{k\le j}(p_{k,t+r}-p_{k,t})\right\rangle\sim e^{-mr}\ . \tag{2.8}$$

The ground state at zero temperature, for $0\le\Delta<\frac{1}{2}$, is the vacuum state

$$|\psi_0\rangle_{T=0}=|p_{\bar{n}}=0,\ n=1,2,\ldots\rangle\ . \tag{2.9}$$

In view of the definition of $p_{\bar{n}}$, Eq. (2.7b), this is simply the statement that there are no domain walls in the system; this is a commensurate phase with $Q_\theta=0$. For $\frac{1}{2}<\Delta\le 1$ and $T=0$, the ground state consists of clockwise domain walls ($\theta_{n+1}-\theta_n=1$) at every bond:

$$|\psi_0\rangle_{T=0}=|p_{\bar{n}}=1,\ n=1,2,\ldots\rangle\ . \tag{2.10}$$

This commensurate phase has $Q_\theta=1$. At $\Delta=\frac{1}{2}$, $T=0$, the kinetic energies of the $p_{\bar{n}}=0$ and $p_{\bar{n}}=1$ excitations are degenerate; an arbitrary number of clockwise domain walls may be placed randomly in the system.

For low temperatures and Δ near the multidegeneracy point $\Delta=\frac{1}{2}$, the free-fermion approximation may be used to establish the existence of a striped incommensurate phase in which the pitch Q_θ varies continuously between 0 and 1.[1,4] In quantum language, Q_θ is the density of fermions ($p_{\bar{n}}=1$ excitations) or, equivalently, the density of clockwise domain walls.

The free energy of a single fermion with wave vector q is given by the mass gap derived perturbatively, to first order, from the one-particle state

$$|\psi_1\rangle_{T=0}=\sum_n |p_{\bar{n}}=P=1;p_{\bar{m}\neq\bar{n}}=0\rangle e^{-ianq} , \tag{2.11}$$

i.e.,

$$m^1(q)=\cos(\Delta a)-\cos(1-\Delta)a-T\cos(qa) . \tag{2.12}$$

To find the critical temperature T_c, simply set $m^1(q)=0$,

$$T_c(q)=\frac{\cos(\Delta a)-\cos(1-\Delta)a}{\cos(qa)} . \tag{2.13}$$

This shows that $q_c(\Delta)=0$, and when $|\frac{1}{2}-\Delta|\ll 1$,

$$T_c(0)\simeq\frac{2\pi}{\sqrt{3}}\left|\frac{1}{2}-\Delta\right| ,$$

which gives the *C-I* critical line. The gap vanishes linearly along this line, i.e., $\nu=1$.

At higher temperatures the *C-I* boundary must be deduced from the longer series for m. According to the free-fermion analysis, there is no singularity in the free energy on the commensurate side of the transition. Thus, in this work, the only way we can predict the *C-I* boundary is by looking at the vanishing of the mass gap.

The series expansions in this paper are derived by means of a connected-diagram technique.[6] In this method the lattice is essentially infinite, as we only calculate quantities which, in the thermodynamic limit, are independent of the size of the system (e.g., the mass-gap and ground-state energy per site). Thus, in contrast to the finite-lattice approach, the wave vector q may take any value.[7]

B. Numerical results

Numerical data are derived from the following quantities:

(1) Thirteenth-order series for the ground-state energy, order parameter, and susceptibility;

(2) Ninth-order series for the mass gap.

Critical points and critical indices are obtained by the *D* log Padé method, and the data points in the various figures represent the average of three or four of the highest-order diagonal and near-diagonal entries of the Padé tables. As an exception, the Kosterlitz-Thouless data are found by using a modified ratio test.

The error bars are set to include the Padé estimates which have been used to calculate the average of a quantity. As such, these errors reflect only the precision of the data, and do not account for the systematic errors characterizing the Padé method. For example, we have ignored the effect of possible confluent singularities.[8]

It is sufficient to study the region $0\leq\Delta\leq\frac{1}{2}$, according to the symmetries

$$H(\beta,\Delta;\theta_n,p_n)=H(\beta,-\Delta;-\theta_n,-p_n) \tag{2.14a}$$

$$=H(\beta,\Delta+k;\theta_n+nk,p_n) , \tag{2.14b}$$

where k is an integer. These symmetries are valid because the sets $\{\theta_n,p_n\}$, $\{-\theta_n,-p_n\}$, and $\{\theta_n+nk,p_n\}$ have identical eigenvalues and satisfy the same commutation relation (1.2).

1. *Lifshitz point, $\Delta=\frac{1}{4}$*

Our identification of ($\Delta=\frac{1}{4}$, $T_c\simeq 0.75$) as the Lifshitz point is supported by the following evidence:

(1) Figure 2 is a plot of the critical points derived from the low-temperature mass gaps [cf. Eq. (2.8)] m_1 and m_2. These masses correspond, respectively, to the free energies of a "light" and "heavy" domain wall [$P=1$ or 2 in Eq. (2.11)]. The solid line is a smooth curve passing through the m_1 critical points, which are shown in Fig. 1. Error bars have been

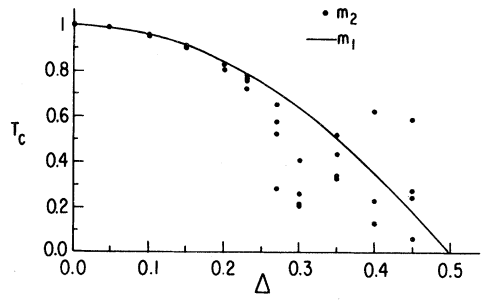

FIG. 2. Critical points derived from the mass gaps m_1 and m_2.

omitted wherever they are smaller than the size of the plotted point. The dots in Fig. 2 represent the m_2 critical points. Instead of averaging over the Padé table, the individual entries are displayed.

For $0 \leq \Delta \leq 0.23$ it appears that both masses predict the same critical point. However, for $0.27 \leq \Delta \leq 0.45$ the m_2 data are scattered. We interpret this erratic behavior as being a consequence of the Padé scheme "demanding" a singularity, and we do not believe the m_2 poles represent phase transitions in this region.

The data of Fig. 2 indicate that a qualitative change in the nature of the transition occurs between $\Delta \sim 0.23$ and ~ 0.27. From this it is reasonable to assert the existence of a Lifshitz point at $\Delta = 0.25$; for $0 \leq \Delta < 0.25$ the distinction between the two types of domain walls is irrelevant, and the transition remains three-state Potts-type, while for $0.25 < \Delta < 0.5$ the heavy domain walls are "frozen out," and a *C-I* transition occurs when m_1 vanishes.

(2) The point $\Delta = \frac{1}{4}$ is singled out by the special symmetry which applies there. Combining Eqs. (2.14), one can show that

$$H(\beta,\Delta;\theta_n,p_n) = H(-\beta,\tfrac{1}{2}-\Delta,-\theta_n-n,-p_n) \; . \tag{2.15}$$

A negative β implies antiferromagnetic couplings ($K_x < 0$) in the x direction [cf. Eq. (1.3)]. Thus (2.15) relates, for example, the critical lines for ($0 \leq \Delta \leq \frac{1}{4}$, $\beta > 0$) to the ones located in the region ($\frac{1}{4} \leq \Delta \leq \frac{1}{2}$, $\beta < 0$). Equation (2.15) also implies that at $\Delta = \frac{1}{4}$ the high-temperature series are even functions of Δ, i.e., the critical properties are independent of the sign of K_x.

Of course, this symmetry property does not prove the existence of a Lifshitz point at $\Delta = \frac{1}{4}$ or any other value of Δ. It merely suggests that $\Delta = \frac{1}{4}$ is the most likely point at which crossover behavior occurs.

(3) Recent analysis[4] of a self-dual version of Eq. (1.1) indicates the special role of $\Delta = \frac{1}{4}$. The Hamiltonian of the self-dual model is given by

$$H_{\rm SD} = -\sum_n \cos(p_n - \Delta)a + \beta \cos(\theta_{n+1} - \theta_n - \Delta)a \; . \tag{2.16}$$

At $\Delta = \frac{1}{4}$, the series for the magnetization and mass gap suggest the exact results

$$\langle D \rangle = (1-\beta^2)^{1/9} \tag{2.17a}$$

and

$$m(q=0) = \frac{\sqrt{3}}{2}(1-\beta) \; . \tag{2.17b}$$

[In the self-dual model, the series for $\langle D \rangle$ reproduces the first 14 terms of the binomial expansion of (2.17a), and all terms in the mass gap of order 2–9 are 0.] Equation (2.17a) displays the exact three-state Potts-model magnetization index,[9] $\beta = \frac{1}{9}$, and (2.17b) is equivalent to the Ising-model mass gap, i.e., $\nu = 1$. The exponents α and γ are also Potts-type. Additional numerical studies indicate that the Lifshitz points of this self-dual model are at ($\Delta = \frac{1}{4}$, $\beta = \pm 1$), and the $\beta = +1$ point is the intersection of a Potts line and two *C-I* lines.

(4) On the basis of universality, one might expect the self-dual and Ostlund Hamiltonians to share some common features. Indeed, based on our assumption that the Lifshitz point is at $\Delta = \frac{1}{4}$, it appears that both models exhibit the same critical indices at this point. These include the high-temperature index ν_H derived from (2.4) ($P = 1$ or 2 gives the same ν_H), and the low-temperature indices ν_1 and ν_2, corresponding to the masses of clockwise ($P = 1$) and counterclockwise ($P = 2$) domain walls [cf. Eq. (2.11)]. Our method of calculating m_2 is invalid at $\Delta = \frac{1}{4}$ because the state defined by (2.11), with $P = 2$, is degenerate with the state consisting of two consecutive domain walls, i.e., $p_{\bar{n}} = p_{\overline{n+1}} = 1$. We cannot predict the critical index of the correct $P = 2$ state (obtained by degenerate-state perturbation theory).

The results are as follows:

$$\nu_1(\tfrac{1}{4}) = 0.946 \pm 0.003 \quad (T_c = 0.7465 \pm 0.0007) \; ,$$
$$\nu_H(\tfrac{1}{4}) = 0.94 \pm 0.01 \quad (T_c = 0.755 \pm 0.002) \; , \tag{2.18}$$

and suggest that perhaps $\nu_1(\frac{1}{4}) = \nu_H(\frac{1}{4}) = \nu_1^{\rm SD}(\frac{1}{4}) = 1$ [cf. (2.17b)]. The determination of the indices is hampered by our ignorance of the exact critical point. For example, if we assume $T_c(\Delta = \frac{1}{4}) = 0.75$, we find $\nu_1(\frac{1}{4}) = 1.00 \pm 0.02$.

Critical indices for the low- (L) and high- (H) temperature ground-state series suggest that these quantities are Potts-type. The results are as follows:

$$\alpha_L = 0.41 \pm 0.05, \quad \alpha_H = 0.497 \pm 0.004 \; ,$$
$$\beta_L = 0.061 \pm 0.005, \quad \beta_H = 0.18 \pm 0.01 \; , \tag{2.19}$$
$$\gamma_L = 1.389 \pm 0.006, \quad \gamma_H = 1.68 \pm 0.02 \; .$$

The exact Potts values[9,10] are $\alpha = \frac{1}{3}$, $\beta = \frac{1}{9}$, $\gamma = \frac{13}{9}$. The high-temperature results deteriorate somewhat near $\Delta = \frac{1}{4}$, no doubt due to the nearness of the Kosterlitz-Thouless line, along which β, γ, and ν are essentially infinite.

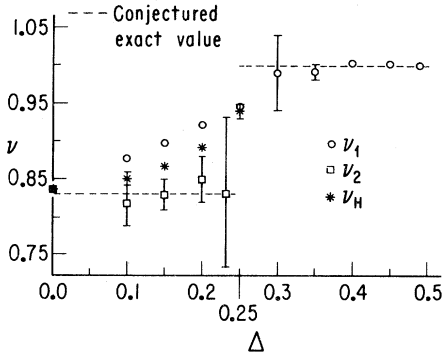

FIG. 3. Mass gap indices; ν_1 and ν_2 refer to low-temperature masses and ν_H is the high-temperature critical index.

The possibility that $\nu=1$ and $\alpha=\frac{1}{3}$ at the Lifshitz point indicates that either hyperscaling is violated, or scaling is anisotropic. Note that in Eqs. (2.3) and (2.8) the mass gap describes correlations in the t direction; these correlation lengths are simply related to the eigenvalues of H. However, the series method used here does not allow us to independently determine the x-direction correlation length or its critical index ν_x.

In the presence of anisotropic scaling, the hyperscaling relation is $\alpha=2-\nu_t-\nu_x$. We can then propose the following classification: The Potts line, $0\leq\Delta<\frac{1}{4}$, is characterized by isotropic scaling, i.e., $\nu_x=\nu_t=\frac{5}{6}$, where $\nu_t=\nu_1=\nu_2=\nu_H$ (a caveat: cf. Fig. 3); scaling is anisotropic at the Lifshitz point, $\Delta=\frac{1}{4}$ with $\nu_x=\frac{2}{3}$ and $\nu_t=\nu_1=\nu_H=1$; scaling is also anisotropic along the *C-I* line, $\frac{1}{4}<\Delta<\frac{1}{2}$, but in this case $\nu_x=\frac{1}{2}$ and $\nu_t=\nu_1=1$ ($\alpha=\frac{1}{2}$ is a prediction of the free-fermion approximation).

This scaling classification is similar to one predicted by a theory of the smectic-*A*-nematic transition in three dimensions,[11] namely, an isotropic line with $\nu_x=\nu_t$, and an anisotropic line with $\nu_x/\nu_t=\frac{1}{2}$, are separated by a special point analogous to the Lifshitz point, but where the anisotropic scaling is given by $\nu_x/\nu_t=\frac{2}{3}$.

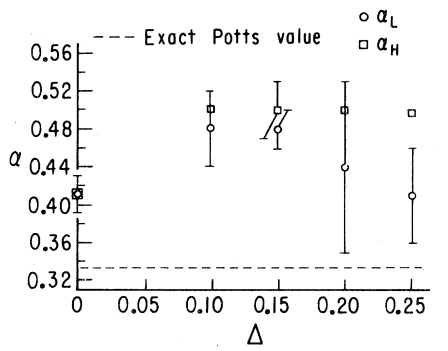

FIG. 4. Low- (○) and high- (□) temperature specific-heat exponents along the Potts line.

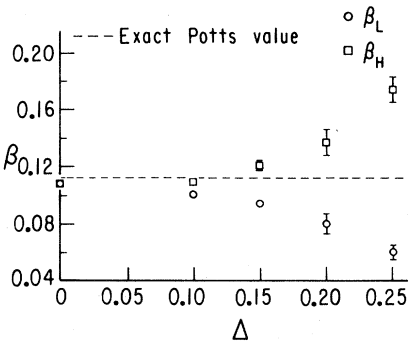

FIG. 5. Order-parameter indices along the Potts line.

2. *Potts line, $0\leq\Delta<\frac{1}{4}$*

For small Δ, the transition is expected to remain three-state Potts-type. Indeed, for $0\leq\Delta\leq\frac{1}{4}$, all of the series predict virtually the same critical point. The critical indices along this line are compared with the conjectured values in Figs. 3–6. In Fig. 3 note the apparent continuous variation of ν_1 and ν_H, whereas ν_2 is quite stable. It is not clear whether or not this variation is merely a consequence of the finite-series approximation.

3. *Commensurate-incommensurate line, $\frac{1}{4}<\Delta<\frac{1}{2}$*

In Sec. II A we derived Eq. (2.13), an expression for the *C-I* critical line, which is valid for low temperatures and $|\frac{1}{2}-\Delta|\ll 1$. The $P=1$ mass series predicts a T_c in agreement with (2.13) for $|\frac{1}{2}-\Delta|\lesssim 0.01$, i.e., $q_c(\Delta)=0$ and $\nu(\Delta)=1$. The ground-state series suggest a larger value of T_c, but the critical indices are erratic and quite small, and hence unphysical. For example, in the region $|\frac{1}{2}-\Delta|\lesssim 0.05$, the magnetization and specific-heat series predict a T_c which is larger than the one derived from m_1, and the indices are given by $\alpha\lesssim 0.07$ and $\beta\lesssim 0.001$, i.e., both quantities approach a con-

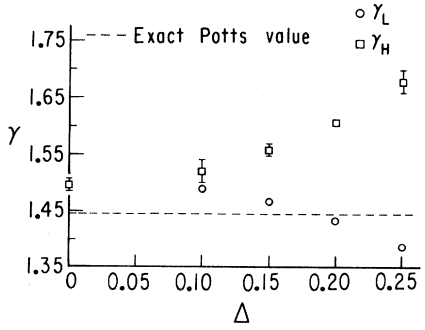

FIG. 6. Susceptibility indices along the Potts line.

stant at the *C-I* transition. This is consistent with the free-fermion picture of the *C-I* transition: The magnetization jumps discontinuously to zero, and the free energy is nonsingular as the *C-I* line is approached from the commensurate side.

We find that this behavior persists at higher temperatures; the mass gap vanishes linearly (cf. Fig. 3) and the critical wave vector remains zero. Poles and critical indices extracted from the ground-state series are erratic and small.

4. *Kosterlitz-Thouless transitions*

The free-fermion approximation provides a correct description of the incommensurate phase at low temperatures and $\Delta \sim \frac{1}{2}$. However, at higher temperatures the domain-wall network becomes unstable to the formation of free dislocations. Applying the dislocation-unbinding theory of Kosterlitz and Thouless,[12,13] one predicts the melting of the I phase to a disordered phase. In the quantum method, the dislocations appear naturally in the context of a next-higher-order fermion approximation.

To determine the incommensurate-liquid critical line, we have assumed that the susceptibility of Eq. (2.2) and the correlation length diverge with an essential singularity, e.g.,

$$\chi \sim e^{A(1-\beta/\beta_c)^{-\sigma}} . \tag{2.20}$$

Since the standard D log Padé method is useful only for algebraic singularities (it also does not appear to work for the logarithm of χ), we have used a ratio test proposed by Rehr.[14] If the series is represented as $\chi = \sum_{n=0}^{\infty} a_n \beta^n$, the asymptotic form of the ratios $R_n = a_n / a_{n-1}$ is

$$R_n = \frac{1}{\beta_c}\left[1+\left[\frac{\sigma A}{n}\right]^{1/(1+\sigma)}\right] . \tag{2.21}$$

The quantities A, β_c, and σ are found by fitting the calculated ratios R_n^{calc} to the form (2.22). This is done by searching for a minimum of the quantity

$$S(A,\beta_c,\sigma) = \sum_n (R_n - R_n^{\text{calc}})^2 n^2 . \tag{2.22}$$

In order to apply this ratio test we must first perform an Euler transformation so that the coefficients are of the same sign:

$$\chi(z;c) = \sum_n \tilde{a}_n z^n, \quad z = \frac{\beta}{1-\beta/c} . \tag{2.23}$$

Although we believe that the Kosterlitz-Thouless line begins at $\Delta = \frac{1}{4}$, the above method has only been successful at one point, $\Delta = \frac{1}{2}$. Choosing $c = -0.31$ in (2.24) a minimum of S is located at

$$\begin{aligned} \beta_c &= 9.3 , \\ \sigma &= 0.56 , \\ A &= 0.58 . \end{aligned} \tag{2.24}$$

This value of σ compares with the renormalization-group prediction,[13] $\sigma = \frac{1}{2}$. The absence of data for any other value of Δ appears to be due to the sensitivity of the transformed series with respect to variations of c.

The mass gap derived from (2.4) should also exhibit an essential singularity at the liquid-incommensurate transition. In addition, the critical wave vector q_c is equal to the pitch of the I phase, exactly at the transition. This is based on a similar result for the self-dual model (2.16). In this case, the incommensurate-liquid transition is a *C-I* transition, and it is possible to calculate the correlation function (2.6) using free-fermion techniques. We find that Q_θ varies continuously with Δ, and is equal to q_c^4.

Thus for $\frac{1}{4} \le \Delta \le \frac{3}{4}$ we expect q_c to vary continuously between 0 and 1. The values of q_c on the liquid-incommensurate line determine the lines of constant pitch in the I phase, as indicated schematically in Fig. 7. Unfortunately, we have not been able to extract reliable values of β_c and q_c from the mass gap series. At present there appears to be no efficient means of dealing with an essential singularity.

III. RELATION TO OTHER WORK

Selke and Yeomans[15] have performed a Monte Carlo analysis of the 2D model, Eq. (1.3). While the qualitative features of the phase diagram deduced in their work agree with ours, there remain some quantitative discrepancies. The one-dimensional quantum model has also been studied by Centen, Ritten-

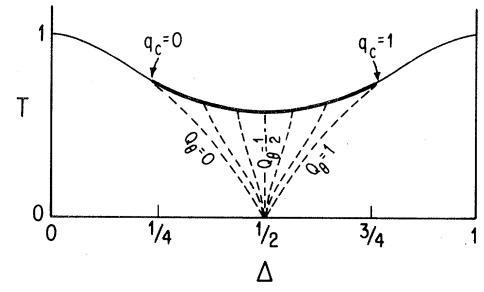

FIG. 7. Dashed lines represent lines of constant pitch in the incommensurate phase. The critical wave vector q_c varies continuously along the heavy dark line. The I phase has been enlarged for clarity.

berg, and Marcu[16] using finite size scaling.

Note added in proof. Recently, Huse and Fisher,[17] Haldane, Bak, and Bohr,[18] and also Schulz[19] have suggested phase diagrams which differ from Fig. 1. Their arguments are based upon the notion that the chiral perturbation is relevant at $\Delta=0$, and are, of course, not fully rigorous. Because of the inaccuracies in the series method, the evidence given here can only suggest, not prove, the validity of Fig. 1. Further work will be needed to decide between the various pictures.

ACKNOWLEDGMENTS

It is a pleasure to thank L. P. Kadanoff and M. P. M. den Nijs for many valuable discussions, and in particular Dr. Kadanoff for a critical review of the manuscript. I have also benefitted from discussions with B. Nienhuis, J. Rehr, and J. Toner. This research was partially supported by a Canadian Natural Sciences and Engineering Research Council (NSERC) Fellowship. This research was supported in part by U.S. Department of Energy Grant No. AC02-81ER-100957A.

---

*Presented as a thesis to the Department of Physics, The University of Chicago, in partial fulfillment of the requirement for the Ph.D. degree.

[1]S. Ostlund, Phys. Rev. B 24, 398 (1981).

[2]M. Jaubert, A. Glachant, M. Bienfait, and G. Boato, Phys. Rev. Lett. 46, 1679 (1981).

[3]J. Villain and P. Bak, J. Phys. (Paris) 42, 657 (1981).

[4]S. Howes, L. P. Kadanoff, and M. P. M. den Nijs, Nucl. Phys. B 215, 169 (1983).

[5]For a review of commensurate-incommensurate transitions see P. Bak, Rep. Prog. Phys. 45, 587 (1982).

[6]L. P. Kadanoff and M. Kohmoto, J. Phys. A 14, 1291 (1981).

[7]Quantum Hamiltonian series for the ANNNI model are studied by M. N. Barber and P. M. Duxbury, J. Stat. Phys. (in press).

[8]The general problem of confluent singularities is reviewed by B. G. Nickel, in *Proceedings of the 1980 Cargèse Summer Institute on Phase Transitions,* edited by M. Levy *et al.* (Plenum, New York, 1981).

[9]M. P. M. den Nijs, J. Phys. A 12, 1857 (1979); B. Nienhuis, E. K. Riedel, and M. Schick, *ibid.* 13, L189 (1980); R. B. Pearson, Phys. Rev. B 22, 2579 (1980); M. P. M. den Nijs, *ibid.* (in press); Phys. Rev. B 27, 1674 (1983); the hard hexagon model, which is believed to be in the three-state Potts model universality class, has been solved exactly by R. J. Baxter, J. Phys. A 13, L61 (1980); J. Stat. Phys. 26, 427 (1981).

[10]J. Black and V. J. Emery, Phys. Rev. B 23, 429 (1981).

[11]J. Toner, Phys. Rev. B 26, 462 (1982); G. Grinstein and J. Toner (unpublished).

[12]J. M. Kosterlitz and D. J. Thouless, J. Phys. C 6, 1181 (1973).

[13]J. M. Kosterlitz, J. Phys. C 7, 1046 (1974).

[14]J. Rehr (unpublished).

[15]W. Selke and J. Yeomans, Z. Phys. B 46, 311 (1982).

[16]P. Centen, V. Rittenberg, and M. Marcu, Nucl. Phys. B 205, 585 (1982).

[17]D. A. Huse and M. E. Fisher, Phys. Rev. Lett. 49, 793 (1982).

[18]F. D. M. Haldane, P. Bak, and T. Bohr (unpublished).

[19]H. J. Schulz (unpublished).